CHAPTER 5

ANN–FLC APPLICATION: SPEED–TRACKING CONTROL OF A DC MOTOR

On the basis of the hybrid artificial neural network and fuzzy logic (ANN–FL) modeling presented in Chapter 4, this chapter walks through a complete design process of an ANN–FL controller for a DC motor system. Results from simulation studies of the newly–designed controller are presented. It is shown that the ANN–FL controller has fast response when the system experiences a load or reference speed change. Also the ANN–FL control system provides perfect speed–tracking control.

5.1 INTRODUCTION

The hybrid ANN–FL modeling technique has been presented in Chapter 4. As an example of application of this method to a simple dynamic system, the dynamics of a direct–current motor will be analyzed and an adaptive controller using the hybrid theory designed. Performance studies of the designed controller will be carried out and a comparison with a PID controller performed. This design procedure will lay a foundation for carrying out stability and control studies for a multi–machine power system in Chapter 8.

Direct–current (DC) motors have found broad applications in industry because of their torque–speed characteristics. The significant features of DC drives include adjustable speed over a wide range, constant mechanical power output, rapid speed change and responsiveness to feedback signals. The speed of a DC motor can be varied by control of the field flux, the armature resistance, or the applied armature voltage. The three most commonly used speed control methods are shunt–rheostat control, armature circuit resistance control, and armature terminal voltage control[5–1].

In this chapter, only the most versatile speed control, that is, speed control by modulating the armature terminal voltage is discussed. In this method alone, speed control can be realized with different control strategies, one of which is PID control. PID stands for Proportional, Integral and Derivative. Such a controller is used to automatically adjust a certain variable so that the output of the controlled process will be held at some set–point. The difference between set–point and the actual measurement of that output is defined as error which is used to initiate the adjustment. This will be further covered in section 5.4 where performance studies are carried out.

5.2 PROBLEM FORMULATION

Let us consider a separately excited DC motor[5–1] as shown in Figure 5.1. The generated speed voltage and the electromagnetic torque developed by the motor can be expressed as,

$$e_a = K\phi_d\omega_m = ki_f\omega_m \tag{5.1}$$

$$T_e = K\phi_d i_d = ki_f i_a \tag{5.2}$$

where,

K and k are constants,

ϕ_d is the direct axis air gap flux that is linearly proportional to the field current i_f,

ω_m is the angular velocity corresponding to the speed of rotation, and

i_a is the armature current.

The voltage equation for the field circuit is expressed as,

$$v_f = L_{ff}\frac{d}{dt}\left(i_f\right) + R_f i_f \tag{5.3}$$

where,

v_f, i_f, R_f and L_{ff} are the terminal voltage, current, resistance and self–inductance of the field circuit, respectively.

The voltage equation for the armature circuit is given by,

$$v_t = e_a + R_a i_a + L_{aq}\frac{d}{dt}\left(i_a\right) \tag{5.4}$$

where,

$v_t, R_{a,}$ and L_{aq} are the terminal voltage, resistance and self–inductance of the armature circuit, respectively.

The dynamic equation for the mechanical system of the motor is expressed as,

$$T_e = ki_f i_a = J\frac{d}{dt}(\omega_m) + B\omega_m + T_L \tag{5.5}$$

or

$$T_e - T_L = J\frac{d}{dt}(\omega_m) + B\omega_m \tag{5.6}$$

where,

J is the combined polar moment of enertia of the load and the rotor of the motor,

B is the equivalent viscous friction constant of the load and the motor,

T_L is the mechanical load torque.

The Laplace transform of the voltage equation (5.4) for the armature circuit can be written as,

$$V_t - E_a = R_a(1+\tau_a s)I_a \tag{5.7}$$

where,

$\tau_a = L_{aq} / R_a$, the electrical time constant of the armature circuit.

The Laplace transform of (5.1) is given by,

$$E_a = L\{kI_f \cdot \omega_m\} \tag{5.8}$$

where L denotes Laplace transform. It is noticed that this is a nonlinear equation. When I_f is constant, it is easy to carry out the transform.

The Laplace transform of (5.6), with a zero initial condition, is given by,

$$T_e - T_L = Js\Omega_m + B\Omega_m \tag{5.9}$$

Fig. 5.1 Schematic Representation of A DC Motor[5–1]

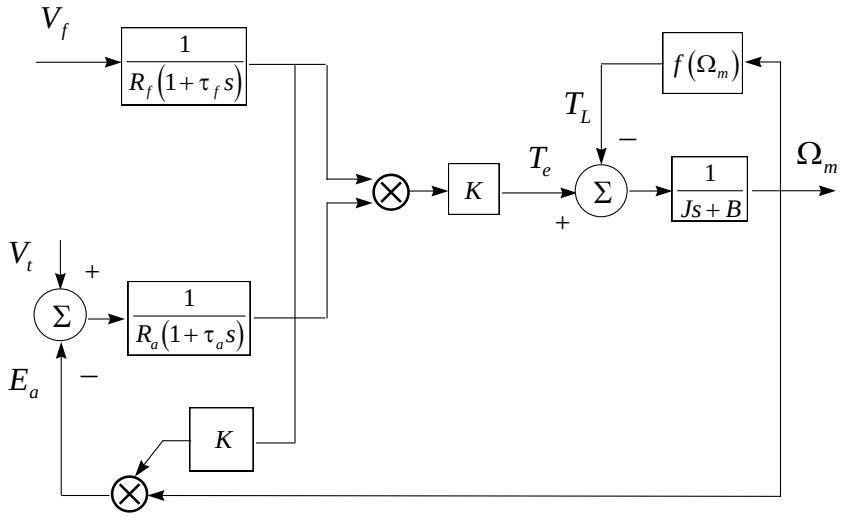

Fig. 5.2 Block Diagram of A DC Motor

Fig. 5.3 Simulation Model of A DC Motor

Figure 5.2 shows the block diagram of the dynamics of a DC motor. Suppose that a 5–hp, 220V, separately excited DC motor has the following parameters: $R_a = 0.5\Omega, L_{aq} = 0.3H, k = 2H, R_f = 220\Omega, L_{ff} = 110H$. The combined constants of the motor armature and the load are $J = 3kg \cdot m^2$ and $B = 0.3kg \cdot m^2 / s$. The field current can be changed by changing the field voltage V_f. Using these data, a simulation model of the motor is constructed as shown in Figure 5.3. Let the step input voltage be 220V. Figure 5.4 shows the dynamic response. The steady state value of the motor speed is 107 rad/s.

5.3 DESIGN OF AN ANN–FL CONTROLLER

5.3.1 Introduction

Based on the hybrid ANN–FL modeling technique presented in Chapter 4, an intelligent control system can be designed for speed control of the DC motor system. To accomplish such a design, the following information, to be discussed in this section, is needed.

(1) A knowledge base that consists of a rule base and a data base. The rule base defines a set of linguistic rules established on expert knowledge of the dynamic behavior of the fuzzy sets used in the rule base. Experience and engineering judgment is incorporated in designing the data base. This will be further covered in the following sections.

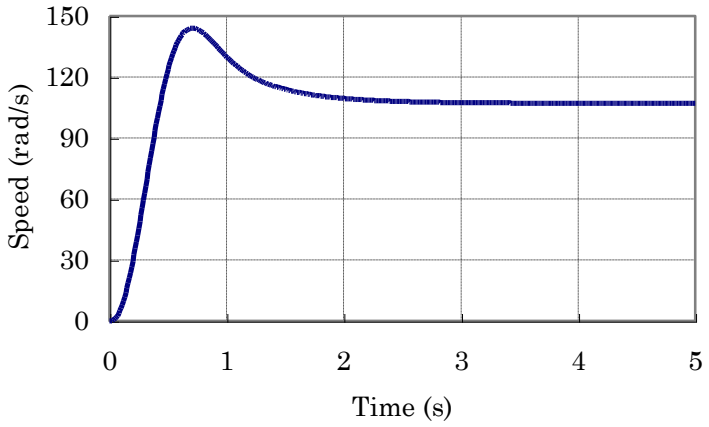

Fig. 5.4 Speed Response of the DC Motor with No Feedback Control

(2) Decision–making logic that imitates human's decision–making processes using fuzzy concepts.

(3) Fuzzification that transforms crisp variables into fuzzy sets. Defuzzification that does the opposite.

(4) An ANN–FL model as defined in Chapter 4.

(5) A training set of data that is collected either from real–world operation or computer simulation of the physical plant.

(6) A training program that implements the above algorithm.

5.3.2 Structure of the ANN–FL Controller

(1) *Linguistic Variables*

The goal of DC motor control in this study is to constrain the speed of the motor to a specified level. Suppose that the speed and its rate of change are accessible

and measurable. These two state variables can serve as inputs to the ANN–FL controller to be designed. The output of the controller is a change to the terminal voltage applied to the terminal of the amarture winding of the DC motor. Suppose that the state variables can be described by the following fuzzy sets, with v=very and m=moderate:

Change_of _speed =

[v_negative, m_negative, negative, positive, m_positive, v_positive]

Rate_of_speed_change =

[v_slow, m_slow, slow, fast, m_fast, v_fast]

The output variable of the controller can be described by a fuzzy set as follows:

Change_of_voltage = [negative, positive]

In fuzzy set theory, it would not matter how beautifully the linguistic variables are named, the control algorithm recognizes only what is happening in the physical process. Therefore, all the above fuzzy sets can be represented by linguistic labels such as negative big(NB), negative medium(NM), negative small(NS), positive small(PS), positive medium(PM), and positive big(PB). That is, these fuzzy variables can be expressed in terms of the corresponding linguistic labels as follows:

$$\Delta\omega = [NB, NM, NS, PS, PM, PB] \tag{5.10}$$

$$\Delta\omega / \Delta t = [NB, NM, NS, PS, PM, PB] \tag{5.11}$$

$$\Delta V = [N, P] \tag{5.12}$$

(2) *Membership Functions*

Suppose that the ranges of change of the fuzzy variables of the DC motor to be controlled are known from design or operational requirements. Then the universe of disclosure of the fuzzy sets can be determined. For example,

$$\Delta\omega = [-30,+30]\,(rad) \tag{5.13}$$

$$\Delta\omega / \Delta t = [-75,+80]\,(rad/s) \tag{5.14}$$

$$\Delta V = [-60,+60]\,(volt) \tag{5.15}$$

Then, membership functions can be assigned to each of the above fuzzy sets, including both of those of the input and output variables. Figure 5.5 – 5.7 show the membership functions for the state variable $\Delta\omega/\Delta t, \Delta\omega$, and the output variable ΔV, respectively. Membership functions for fuzzy sets $A_{i2},\ldots,A_{i5}(i=1,2)$ are expressed by Gaussian function which takes the form of (5.16), and membership functions for fuzzy sets $A_{i1}, A_{i6}, B_i(i=1,2)$ are expressed by a Bell function which takes the form of (5.17). Table 5.1 shows a rule base for the ANN–FL controller, where $A_{ij}, B_i(i=1,2; j=1,2,\ldots,6)$ are membership functions.

$$f(x,\sigma,c) = e^{-\left\{\frac{x-c}{\sqrt{2}\sigma}\right\}^2} \tag{5.16}$$

$$f(x,a,b,c) = \frac{1}{1+\left\{\frac{x-c}{a}\right\}^{2b}} \tag{5.17}$$

The parameters of these membership functions will be determined in a training process with data obtained from simulations of the DC motor with PID control.

(3) *Structure of the ANN–FL Controller*

A five–layer feedforward network, with two inputs and one output, is designed as shown in Figure 5.8. The universe of discourse of each input variable is initially divided into six segments. There are six membership functions for each of these variables. As has been mentioned earlier, each membership function is labeled with $A_{ij}\left(i=1,2;\, j=1,2,\ldots,6\right)$. The output variable has two membership functions, labeled as $B_i\left(i=1,2\right)$. Definitions of these linguistic labels are given by (5.10) and (5.12).

The generalized Bell–curve function is chosen as the membership function of the output variable. Initially, A_{11} and A_{21} were represented by a Z–shaped membership function and A_{16} and A_{26} by a S–curve membership function. After training and simulation comparison, they are replaced with the generalized Bell–curve membership function. The rest of the membership functions are represented by Gaussian–curve function.

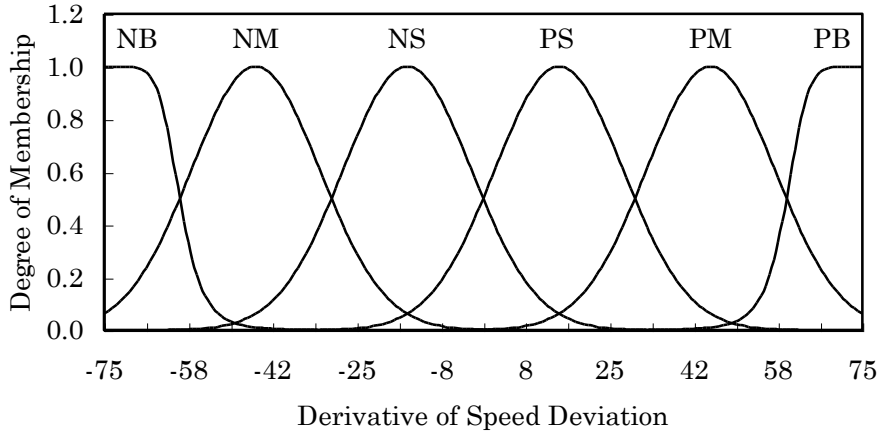

Fig. 5.5 Membership Functions for State Variable $\Delta\omega / \Delta t$

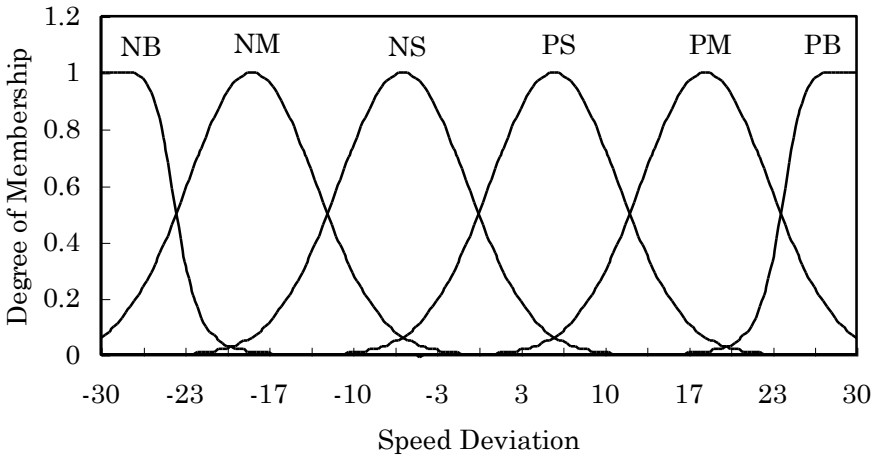

Fig. 5.6 Membership Functions for State Variable $\Delta\omega$

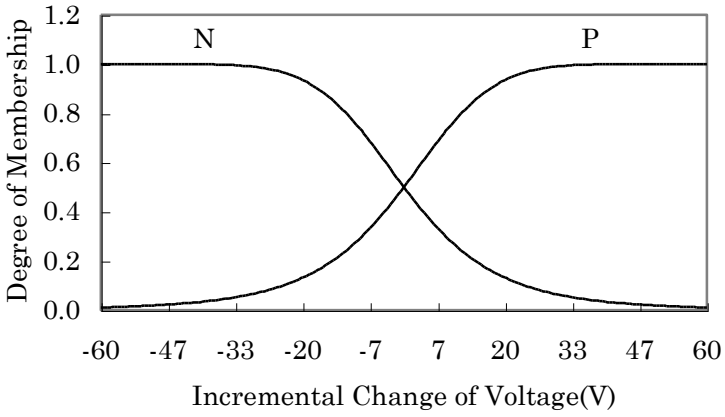

Fig. 5.7 Membership Functions for Output Variable ΔV

Table 5.1 Rule Base of the ANN–FL Controller

$\Delta\omega$ / ΔV / $\Delta\omega/\Delta t$	A_{11}	A_{12}	A_{13}	A_{14}	A_{15}	A_{16}
A_{21}	B_2	B_2	B_2			
A_{22}	B_2	B_2	B_2			
A_{23}	B_2	B_2	B_2			
A_{24}				B_1	B_1	B_1
A_{25}				B_1	B_1	B_1
A_{26}				B_1	B_1	B_1

(4) *Collection of Training Data*

A number of simulation studies of the DC motor dynamic system, shown in Figure 5.3, are carried out, simulating different load disturbances. These disturbances cause the changes of the state variables in their corresponding ranges as specified in (5.13) and (5.14). The available voltage change of the power source is specified in (5.15). The results from the simulations are recorded in Table 5.2. The first row in Table 5.2 is the speed deviation relative to reference speed. The first column is the derivative of the speed deviation. The numbers in Table 5.2 are the incremental voltage change relative to the normal terminal voltage which is 220 volts. These data will be used for training the ANN–FL controller. For design purpose, a near–optimal PID controller is used in the simulation to obtain the desired performance of the system. The parameters of the PID controller will be given later in this chapter when performance studies are carried out.

(5) *Supervised learning of the ANN–FLC system*

Up to this point, the ANN–FLC has an initial set of values for the parameters of the membership functions, given the fuzzy partitions and fuzzy logic rules. The task of a supervised learning scheme is to optimally adjust these parameters so that the controller will perform optimally no matter what the operating point is. Backpropagation [5–2] is used for the learning. A training program has been written using MATLAB and its Fuzzy Logic Toolbox

functionality. Another advantage of using this toolbox is that a newly–designed fuzzy controller can be easily interfaced with the TSSP package, see Chapter 7 of this thesis. The objective of the learning process is to find an optimal set of parameter values for the node functions in the network of Fig. 5.8 so that the total error function,

$$E_p = \frac{1}{2}\sum_{j=1}^{No}\left(t_{pj} - y_{pj}^{L}\right) \tag{5.18}$$

is minimized. Detailed learning rules have been presented in Section 4.4 of this thesis. There are 34 parameters for the membership functions, and 18 weights to be adjusted. The training set of data is given in Table 5.2. There are a total of 127 pairs of training patterns.

As the input variables are fuzzy to the controller, the stopping criterion for training doesn't have to be high. That means, training can be stopped at 1000 epochs or if the total error is less than, say, 0.2. After 1000 epochs of training, the network of the ANN–FL controller converges to a set of parameters that determine the membership functions and weights. These membership functions are displayed as per Figures 5.9–5.11. Figure 5.12 displays the RMSE(root mean squared error) curve of the training process. An adaptive procedure is used for changing the step size during training. The true step sizes used in the training are displayed in Figure 5.13. The reason for using a varying step size in each iteration is to ensure that the error function will not increase.

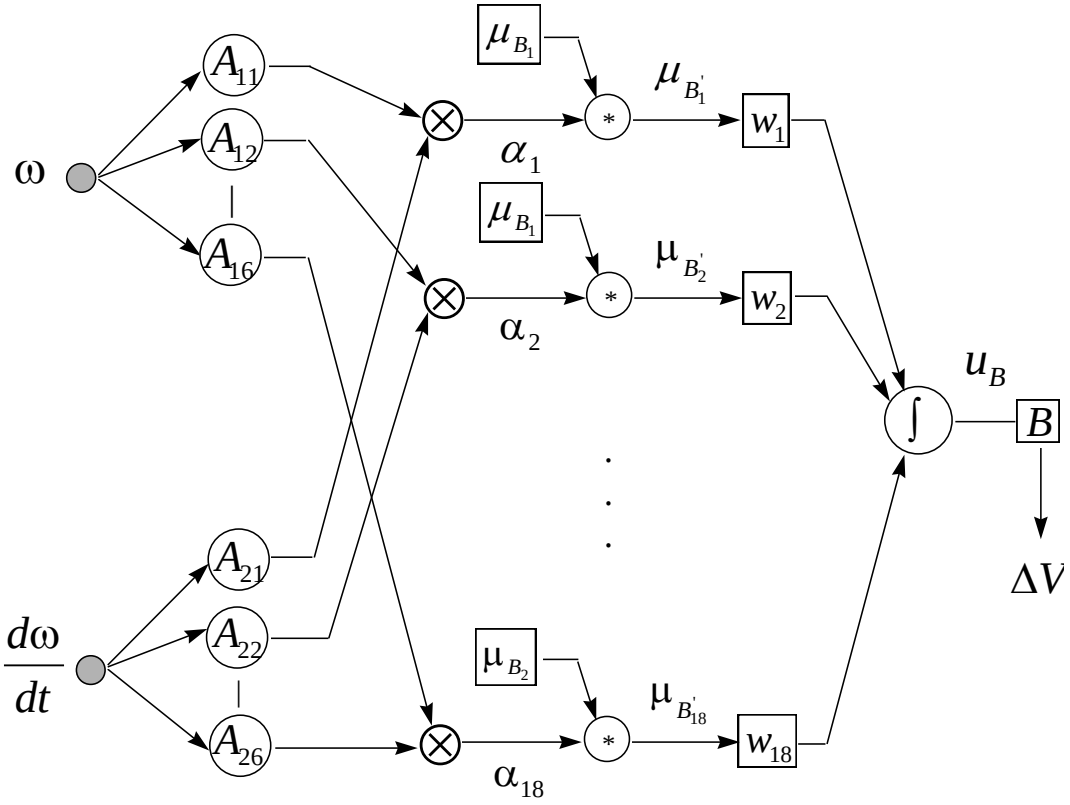

Fig. 5.8 An ANN-FL Controller for DC Motor Control

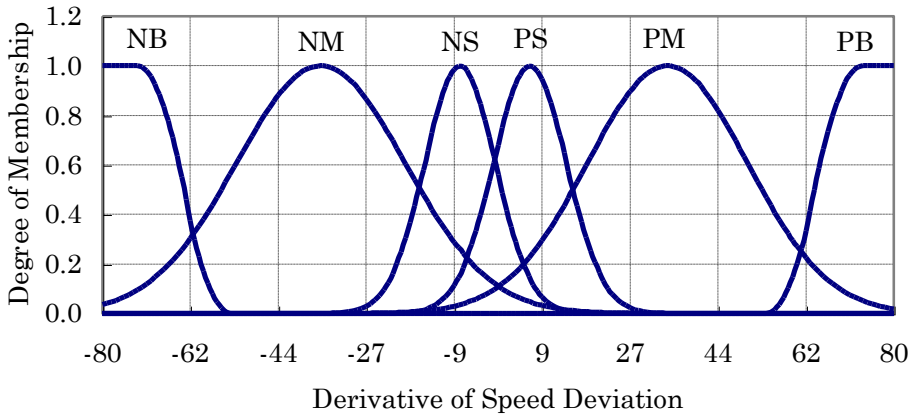

Fig. 5.9 Membership Functions for State Variable $\Delta\omega / \Delta t$

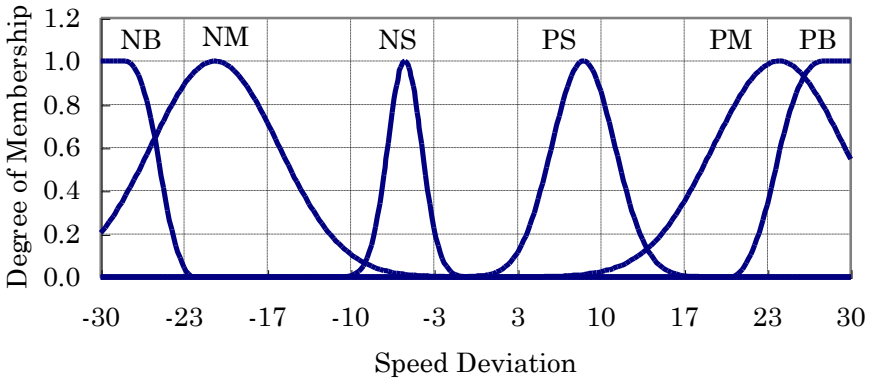

Fig. 5.10 Membership Functions for State Variable $\Delta\omega$

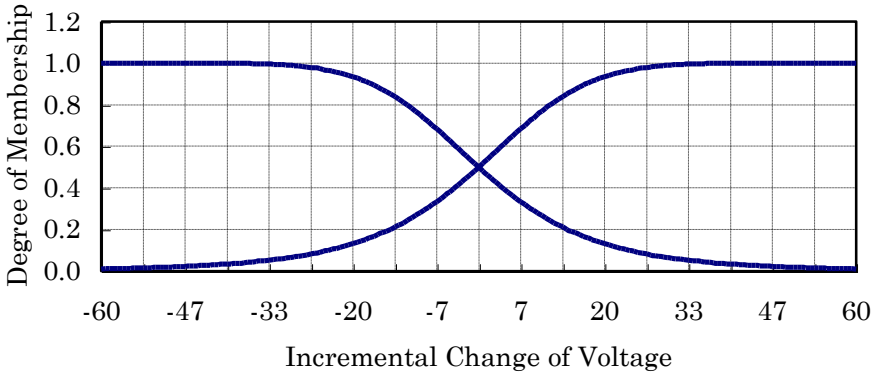

Fig. 5.11 Membership Functions for Output Variable ΔV

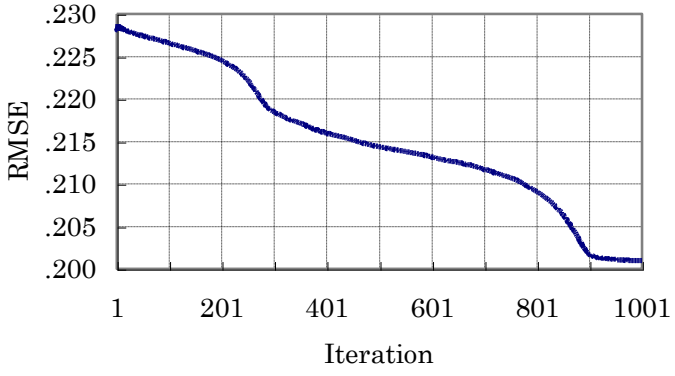

Fig. 5.12 RMSE Curve vs. Epochs

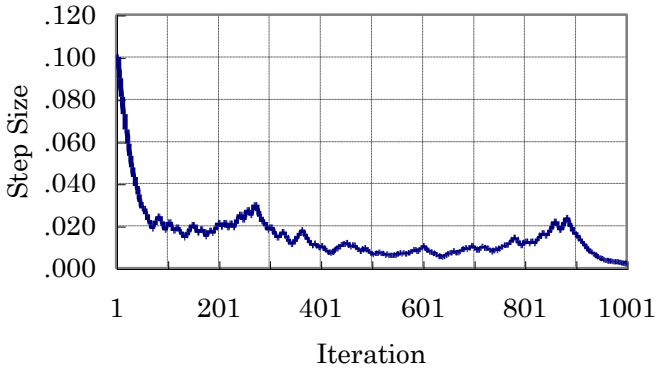

Fig. 5.13 Step Sizes vs. Epochs

Table 5.2 Training Data as Obtained from Simulation Studies

Δω / ΔV / Δω / Δt	-28	-24	-19	-14	-9	4	-1	0	1	4	9	14	19	24	28
-75	60	55	50	46	42	38	34	30							
-62	55	50	46	41	37	33	29	25							
-49	50	46	40	36	32	28	24	20							
-36	46	41	36	30	27	23	19	15							
-23	42	37	32	27	20	16	13	10							
-10	38	33	28	23	16	10	7.5	5							
-1	34	29	24	19	13	7.5	2.5	1.25							
0	30	25	20	15	10	5	1.25	0	-1.25	-5	-10	-15	-20	-25	-30
5								-1.25	-2.5	-7.5	-13	-19	-24	-29	-34
13								-5	-7.5	-10	-16	-23	-28	-33	-38
28								-10	-13	-16	-20	-27	-32	-37	-42
41								-15	-19	-23	-27	-30	-36	-41	-46
54								-20	-24	-28	-32	-36	-40	-46	-50
67								-25	-29	-33	-37	-41	-46	-50	-55
80								-30	-34	-38	-42	-46	-50	-55	-60

5.4 PERFORMANCE EVALUATION

5.4.1 Introduction

As hardware and software technology has advanced a great deal in the last few years, digital control techniques have become more affordable and indispensable with the growing requirements for higher supervisory capability and better control performance in some control systems. For DC motors to achieve speed–tracking control, some adaptive control algorithms are required. Usually they are rather complicated and require a computer to do the job. Therefore, almost all applications of adaptive control to motor drives still remain in computer simulation studies for this reason[5–4]. The following study shows that a hybrid artificial neural network and fuzzy–logic(ANN–FL) controller needs only a simple and fast algorithm, once it is designed. This may open the door for developing fast and economical adaptive controllers for motor drives in the future.

In this section, a number of simulation studies will be presented of the DC motor dynamic system controlled by either a PID controller or the newly–designed ANN–FL controller. The gains of the PID controller are tuned to their optimal values at the normal operating point of the DC motor. In order to carry out a fair comparison, the two controllers will be kept unchanged during the entire simulation studies that follow. The investigation addresses three operating conditions, i.e., (1) operating at normal conditions with different reference speeds; (2) operating at a speed of 110 radians per second

or 525 revolution per minute, experiencing a load change or an excitation voltage change[5–4]; and (3) tracking a pre–specified trajectory[5–5].

5.4.2 Step Response with Different Reference Speeds

From earlier simulation studies, it is known that the DC motor under study operates at 107 radians per second at normal terminal voltage of 220 volts without any feedback control. When the DC motor is required to operate at another speed, it is necessary to have some sort of feedback control such as PID control. The PID controller used here has fixed design gains which are determined for a specific operating condition. Assume now that the DC motor operates at different set–points of speed, say from 70–130 radians per second. Extensive simulation studies were carried out and only a fraction of the obtained results are presented here. Figure 5.14(a) shows the situation where the reference speed, ω_{ref} , is 90 radians per second as applied in the simulation model of Fig. 5.3. By controlling the SWITCH, two step responses corresponding to the PID and the ANN–FL controller were obtained. By increasing the step input to 130 rad/s and following the same procedure, another two step responses were obtained as shown in Fig. 5.14(b). It can be concluded that the PID controller outperforms the ANN–FL controller for step responses.

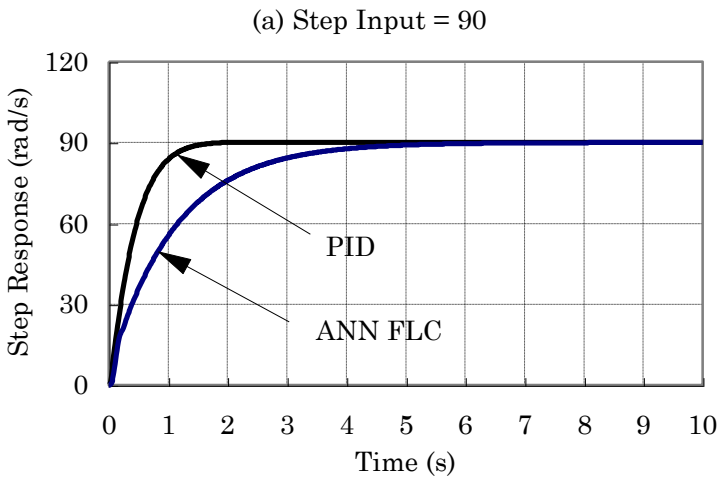

Fig. 5.14(a) Response of PID and ANN–FL Control to A Step Input of 90 rad/s

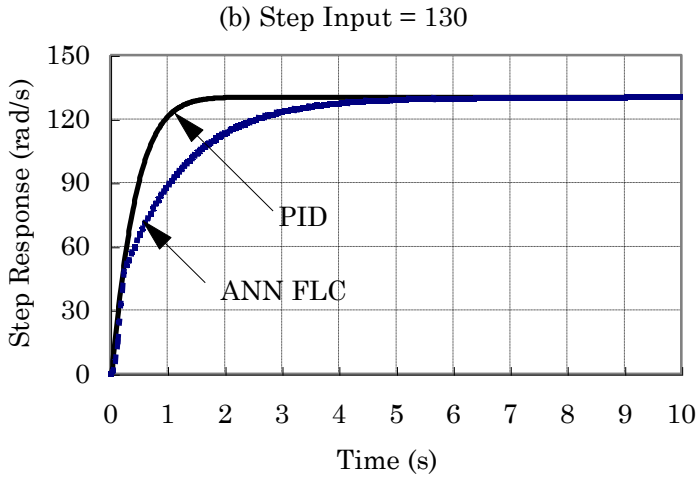

Fig. 5.14(b) Response of PID and ANN–FL Control to A Step Input of 130 rad/s

5.4.3 Different Disturbances

Two situations are considered, i.e., load torque disturbance and field voltage change. Load torque variation is present in any motor drive system, when a motor experiences a load torque increase, the rotor speed decreases. When the load torque decreases, the motor speed goes in the other direction. However, speed response to load torque disturbance is responsive when a feedback control is present. Field voltage variations result in a field current change which causes the emf change. In the end, it causes speed change.

Suppose that the DC motor is operating at a normal speed of 110 radians per second. Two scenarios were studied in this section for demonstrating the performance difference of the two controllers when the system withstands a certain disturbance. Scenario #1 involves load torque disturbance. Let a periodical load disturbance, shown in Fig. 5.15(a), be applied to the summation box S1 of the simulation model of the DC motor, shown in Fig. 5.3. Figure 5.15(b) shows the speed response of the motor to the disturbance, with the PID controller as feedback control. In this case the maximum speed ripple is 0.55 percent. Figure 5.15(c) shows the situation with the ANN–FL controller. The maximum speed ripple is now only 0.1 percent. Figure 5.16 shows a detailed comparison of the speed responses shown in Figs. 5.15(b) and 5.15(c). Note that the time–axis is stretched out so that transient details of the two controllers can be readily seen.

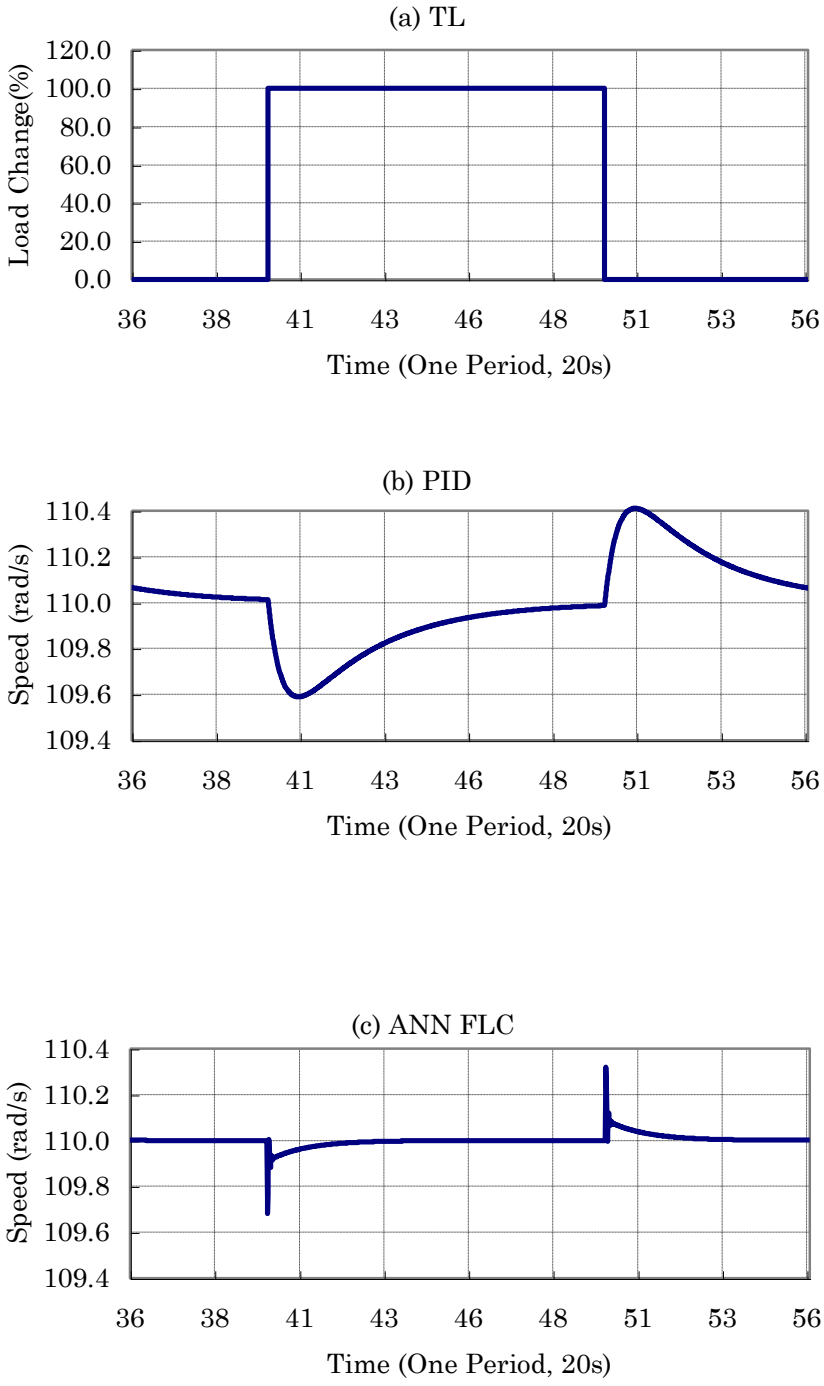

Fig. 5.15 Performance Comparison of ANN–FL vs. PID Control, with A Periodical Load Disturbance Applied

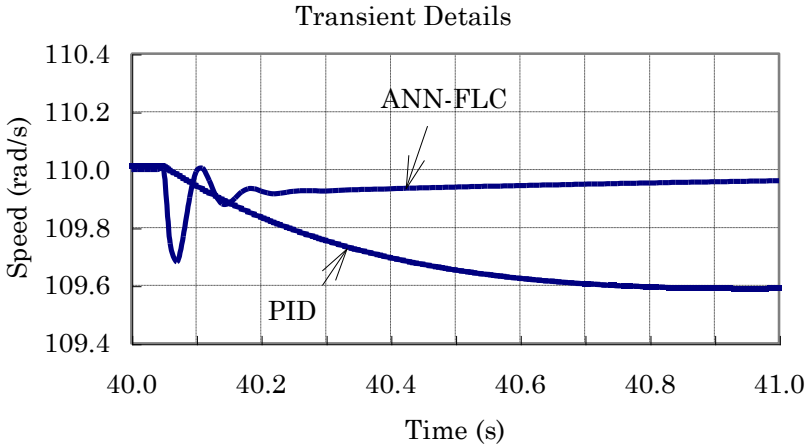

Fig. 5.16 Window Graphic Showing Transient Details in Figs. 5.15(b) & (c)

Scenario #2 involves field voltage change. A periodical voltage disturbance, shown in Fig. 5.17(a), is applied to the summation box S2 of Fig. 5.3. Figures 5.17(b) & (c) show the speed responses of the system with the ANN–FL controller as feedback control. The maximum speed fluctuations are 6, and 1 percent, respectively. Figure 5.18 shows the transient details of the two responses in this case.

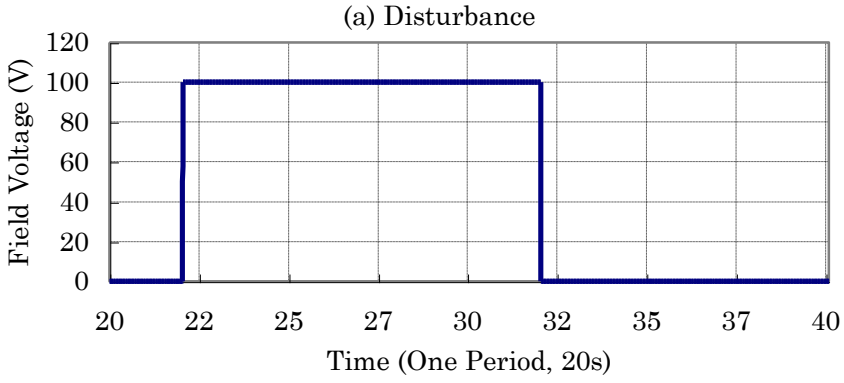

Fig. 5.17(a) A Periodical Field Voltage Disturbance

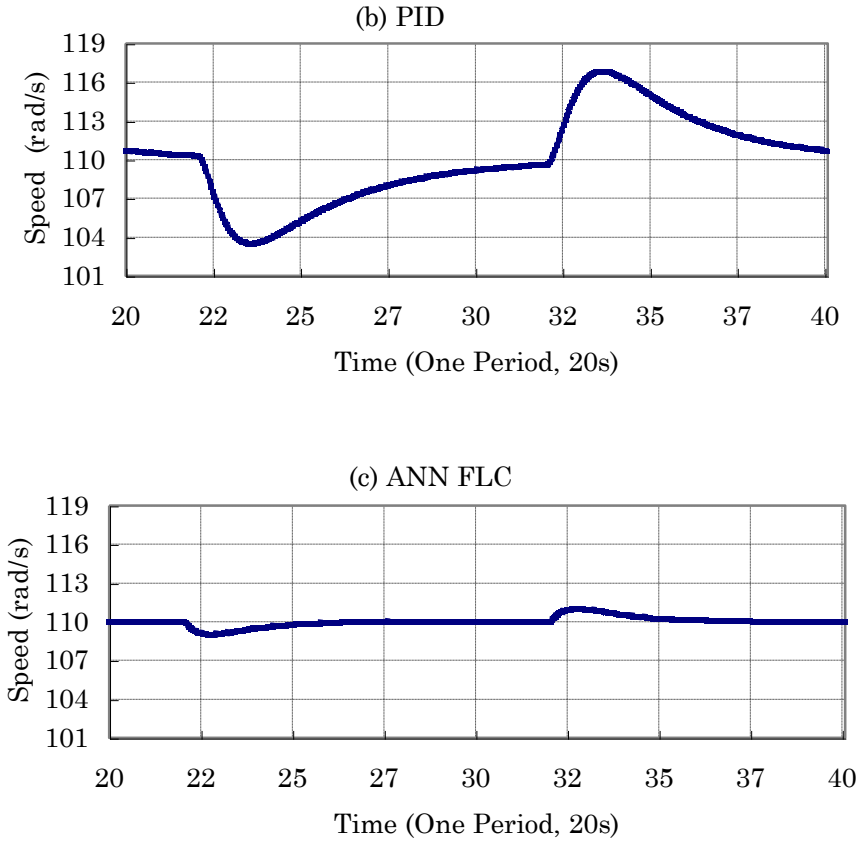

Figs. 5.17(b)(c) Performance Comparison of ANN–FL vs. PID Control Responding to the Disturbance of Fig. 5.17(a)

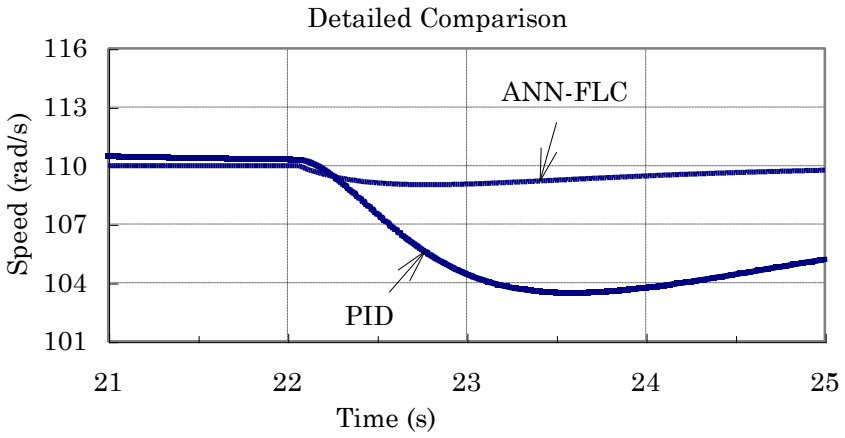

Fig. 5.18 Window Graphic Showing Transient Details in Figs. 5.17(b) & (c)

5.4.4 Trajectory Control

The objective of this simulation study is to demonstrate which of the two controllers can drive the DC motor to follow a pre–specified trajectory more closely. Suppose that the pre–specified speed trajectory is defined by

$$\omega_{ref} = 10\sin(2\pi f_1 t) + 16\sin(2\pi f_2 t) \qquad (5.19)$$ where

$f_1 = ¼\,Hz,\ \ f_2 = ⅐\,Hz$ and $t = 30\,s$.

The simulation was carried out as follows. First, the pre–specified trajectory was computed and sampled with a sampling time step of 0.01 second over a time interval of [0, 30]. Then, it was used as the reference speed, ω_{ref}, in the simulation, using the model of Fig. 5.3. Two simulations were performed using either the PID or the ANN–FL controller. Figure 5.19(a) illustrates the situation where the PID is used. It can be seen that there is a maximum of 15 percent discrepancy between the desired speed and the actual response. Note that the manipulated variable is the output of the controller which is the input to the DC system. This variable is restricted in the range $(-60,+60)$ volts.

Figure 5.19(b) illustrates the case where the ANN–FL controller is used. It produces perfect speed–tracking control. The manipulated variable is also shown in the graphic. Several other different types of reference trajectories were simulated(results not shown). In each of these simulations, the newly–designed ANN–FL controller demonstrated much superior performance.

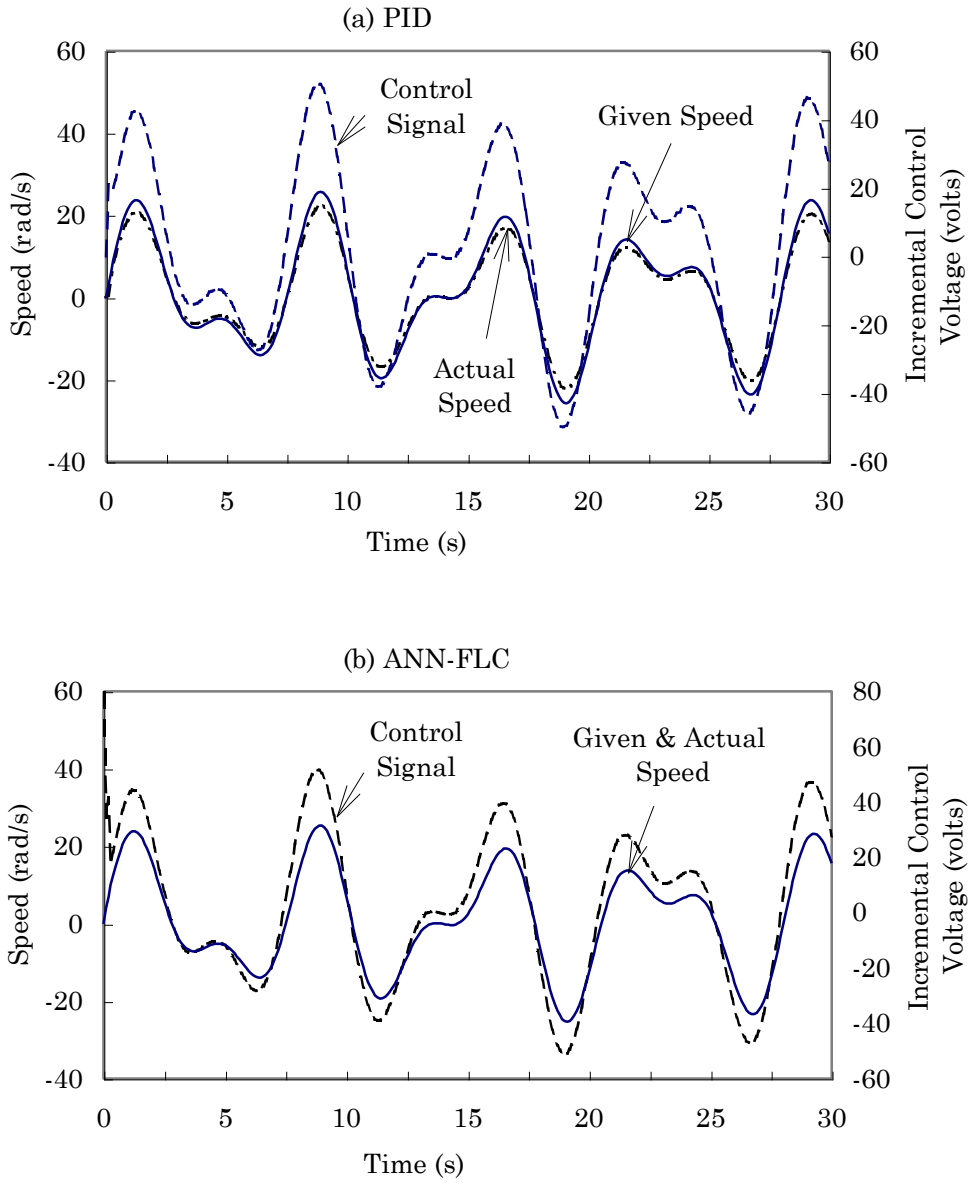

Fig. 5.19 Trajectory Tracking Control of the DC Motor by

(a)PID controller or (b)ANN–FL Controller